

# A SIMULTANEOUS DYNAMIC OPTIMIZATION APPROACH FOR NATURAL GAS PROCESSING PLANTS

J. Ignacio Laiglecia<sup>1</sup>, Rodrigo Lopez-Negrete<sup>2</sup>, M. Soledad Diaz<sup>1</sup>, Lorenz T. Biegler<sup>2</sup>

<sup>1</sup>Planta Piloto de Ingenieria Quimica, Universidad Nacional del Sur, CONICET.  
Camino La Carrindanga km 7, 8000 Bahia Blanca, ARGENTINA

<sup>2</sup>Department of Chemical Engineering, Carnegie Mellon University  
Pittsburgh, PA 15213

## *Abstract*

In this work we address dynamic optimization of natural gas processing plants through the use first principle models and full discretization of both control and state variables. The optimization problem includes rigorous models for cryogenic countercurrent heat exchangers with partial phase change, separation tanks, distillation columns and turboexpanders. Thermodynamic predictions are made with a cubic equation of state. The partial differential algebraic equation system is transformed into ordinary differential-algebraic equations (DAEs) by applying the method of Lines for the spatial coordinate in cryogenic heat exchangers. The resulting optimization problem is formulated and solved by applying orthogonal collocation on finite elements, and the large-scale Nonlinear Programming (NLP) problem is solved with a Newton-based Interior Point method. The objective is to switch between operating modes to minimize the offset between current ethane recovery and a set point value. Numerical results provide temporal and spatial profiles of controlled and manipulated variables, while fulfilling specific path constraints associated to ethane extraction processes. In particular, the tight integration between process units as well as path constraints has been efficiently handled with low computational time.

## *Keywords*

Simultaneous Dynamic Optimization, Heat exchanger with phase change, Natural Gas Plant.

## **Introduction**

Advances in the development of large-scale optimization algorithms as well as in hardware, have allowed addressing dynamic optimization of entire plants with rigorous models. In particular, natural gas processing plants are examples of highly energy integrated cryogenic processes, with numerous path constraints in transient states. These plants provide ethane as raw material for olefin plants, as well as methane for gas sales, LPG and gasoline. Ethane yield must be high, while minimizing energy consumption and complying with environmental regulations; these are related to carbon dioxide emissions and maximum carbon dioxide content in the residual gas injected to the pipeline. Additional path constraints involve keeping carbon dioxide solubility conditions in the upper stages of the demethanizer column. Mandler (2000)

presented Air Products' dynamic modeling efforts since 1990 for analysis and control of cryogenic liquefied gas plants (LNG). Dynamic optimization models have been proposed for cryogenic columns (Cervantes et al., 2000; Diaz et al., 2003; Raghunathan et al., 2004) and cryogenic heat exchangers (Rodriguez and Diaz, 2007). Vinson (2006) presented recent advances in air cryogenic separation. Finally, Rodriguez et al. (2010) proposed a dynamic model for an entire natural gas plant with a simultaneous optimization approach.

Simultaneous dynamic optimization approaches have seen considerable development over the last two decades. Here, both the discretized differential-algebraic equation (DAE) model and the optimal control problem are formulated as a single nonlinear programming (NLP) problem. In particular, the DAEs are discretized to a set of algebraic equations over finite elements in time, often using implicit Runge-Kutta (IRK) methods, such as

orthogonal collocation on finite elements. Moreover, with the development of large-scale nonlinear programming solvers, a number of advantages can be realized. A key feature of the simultaneous approach is that embedded solution of the DAE model is no longer required. Moreover, exact first and second derivative information for the NLP are readily obtained from the algebraic equations resulting from the discretization. The simultaneous dynamic optimization approach is reviewed in Biegler (2010), where it is also compared with competing dynamic optimization strategies. In particular, this approach has been demonstrated to be well-suited to address highly integrated processes with numerous path constraints (Biegler and Zavala, 2008).

In this work, we propose a simultaneous dynamic optimization framework for changing between steady states to maximize ethane recovery in the cryogenic sector of a natural gas plant. The problem includes first principle models for separation tanks, turboexpanders, distillation columns and countercurrent shell and tube heat exchangers with partial phase change. The Soave Redlich Kwong (SRK) equation of state (Soave, 1972) provides thermodynamic predictions for vapor-liquid equilibrium and carbon dioxide solubility predictions. These distributed parameter models are spatially discretized by the Method of Lines (Schiesser, 1991). The resulting optimization problem subject to the DAE system is then discretized by orthogonal collocation on finite elements in AMPL and solved with IPOPT, a Newton-based Interior Point method (Wächter and Biegler, 2006). To achieve enhanced product recovery, this approach has enabled optimal profiles for the main operating variables to be obtained with particularly low CPU times.

## Natural Gas Plant description

Turboexpansion processes are currently the most efficient ones for ethane extraction from natural gas mixtures. Ethane is later provided as raw material for olefin plants. Methane is delivered as sales, with LPG and gasoline as the remaining products. The cryogenic sector, which is shown in Fig. 1, is the most energy intensive part in a natural gas processing plant. The feed gas is cooled by heat exchange with the demethanizer top product in cryogenic heat exchangers (HE1 and HE2), and with side and bottom distillation column reboilers. After heat integration, both streams are mixed and sent to a high pressure separator (HPS). The vapor stream is expanded through a turboexpander (TE) to achieve the low temperatures required for demethanization. The liquid stream from the HPS enters the demethanizer at its lowest feed point. The top product has mainly methane and nitrogen, while higher hydrocarbons are obtained in the bottom product. Carbon dioxide, which has intermediate volatility between methane and ethane, distributes between the top and bottom streams.

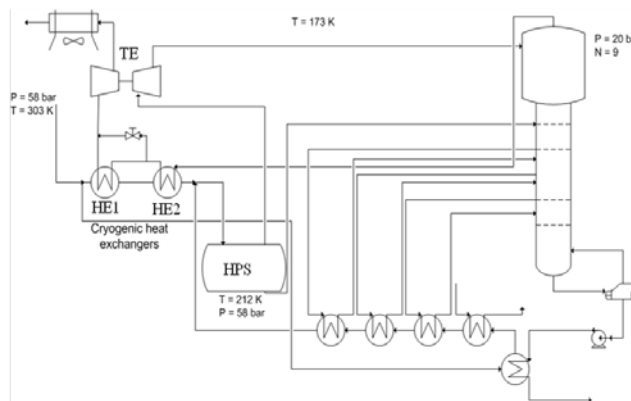


Figure 1. Cryogenic sector in basic turboexpansion process

Cryogenic conditions in the upper stages of the demethanizer column may produce carbon dioxide precipitation, which must be avoided. The top product, residual gas, is used to cool the feed gas and it is then recompressed to the pipeline pressure, and distributed for sale. The bottom product from the demethanizer can be further processed to obtain ethane, propane, butane and gasoline. Ethane then undergoes further carbon dioxide removal prior to its delivery as raw material for ethylene plants.

## Mathematical modeling

A brief description of main features for process unit models is given below.

### *Cryogenic heat exchangers with phase change*

The main simplifying assumptions for countercurrent heat exchangers with partial phase change (HE2, in Fig. 2) are thermodynamic equilibrium between the vapor and liquid phases. However, they can have different velocities, and one dimensional flux. A simple scheme of the cryogenic heat exchanger is shown below.

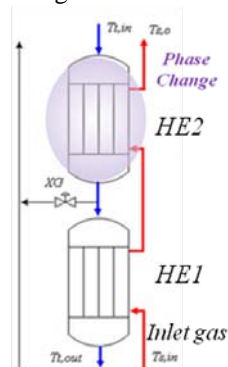


Figure 2. Cryogenic heat exchanger configuration

Thermodynamic predictions are made with the SRK equation of state (Soave, 1972). To transform the partial differential algebraic equation system describing this distributed parameters problem into a DAE, we have applied the Method of Lines, using backward finite differences. In this system, we have selected the fraction of

residual gas flow rate through the bypass valve between HE1 and HE2 as an optimization variable (XG in Fig. 2), as it is used to achieve a desired outlet natural gas temperature to the high pressure separator. The top heat exchanger where partial natural gas condensation takes place (HE2) has been modeled with 6 cells, while the heat exchanger where only sensible heat is exchanged (HE1) is modeled with 10 cells. A detailed description for the cryogenic system model is given in Rodriguez and Diaz (2007) and Rodriguez (2009). To avoid temperature crosses the following constraints have been included for each cell:

$$Ts_k - Tt_{k+1} \geq \Delta T_{min}; k = 1, \dots, N_{cells} - 1$$

$$Ts_k - Tt_{IN1} \geq \Delta T_{min}; k = N_{cells}$$

where  $Ts_k$  denotes the shell temperature in cell  $k$  and  $Tt_{k+1}$  is the corresponding tube side temperature. Additional constraints ensure monotonic temperature profiles along countercurrent heat exchangers:

$$Ts_{m,IN} \geq Ts_{m,1}; m = 1, 2$$

$$Ts_{m,i} \geq Ts_{m,i+1}; i = 1, \dots, N_{cells}; m = 1, 2$$

$$Tt_{m,i} \geq Tt_{m,i+1}; i = 1, \dots, N_{cells}; m = 1, 2$$

$$Tt_{m,N_{cells}m} \geq Tt_{m,IN}; m = 1, 2$$

#### High pressure separator

The model includes an overall dynamic mass balance and geometric equations relating liquid content in the tank to liquid height and liquid flowrate as a function of pressure drop over the liquid stream valve. Detailed equations are presented in Rodriguez and Diaz (2007) and Rodriguez (2009).

#### Turboexpander

The turboexpander is represented with a static model due to its fast dynamics. It is the core unit in cryogenic natural gas processing plants, as it allows achieving low temperatures required for methane/ethane separation. It is modeled as an isentropic expansion, corrected by the expander efficiency. Residual entropy has been calculated with the SRK equation of state. The procedure proposed in GPSA Engineering Data Book (2004) for turboexpander calculation has been implemented and the equation oriented approach efficiently avoids the iterative routine.

#### Demethanizing column

The demethanizer model includes dynamic energy and component mass balances at each stage and equilibrium calculations with SRK equation of state and hydraulic calculations, leading to an index one model. To avoid operating conditions that produce carbon dioxide precipitation in the upper section of the column, additional path constraints on carbon dioxide fugacities have been formulated. They are derived from the isofugacity criterion for phase equilibrium and impose current CO<sub>2</sub> fugacity in the vapor phase be at most 80% of the solid fugacity, at each stage  $i$ :

$$\overline{f_{i,CO_2}^V} \leq 0.80 \overline{f_{i,CO_2}^S},$$

which can be calculated with low computational effort in a simultaneous approach as:

$$\overline{f_{i,CO_2}^V} = y_{i,CO_2} P_i \overline{\phi_{i,CO_2}^V}$$

where fugacity coefficients for pure carbon dioxide and in the vapor mixture are calculated with the SRK equation of state at each stage. Further details can be found in Diaz et al (2003).

#### Optimization algorithm

After discretization, the resulting NLP problems are represented in the general form,

$$\text{Min } F(x), \text{ s.t. } c(x) = 0, x \geq 0$$

where  $F(x)$  and  $c(x)$  represent the objective and constraint functions, and  $x$  are all of the discretized state and control variables. The IPOPT solver handles the bound constraints through logarithmic barrier terms added to the objective function and solves the following barrier problem:

$$\text{Min } \phi(x) = F(x) - \mu \sum_{i=1}^n \ln(x^{(i)}), \text{ s.t. } c(x) = 0$$

where  $x^{(i)}$  denotes the  $i$ -th component of vector  $x$  and  $\mu$  is the barrier parameter. Solving a sequence of barrier problems as  $\mu \rightarrow 0$  results in an efficient strategy to solve the original NLP. The solution of the barrier problems, for fixed  $\mu$ , is obtained by solving the following Karush-Kuhn-Tucker (KKT) conditions:

$$\nabla F(x) + \nabla c(x) \lambda - \nu = 0$$

$$c(x) = 0$$

$$X\nu = \mu e$$

Here  $X = \text{diag}(x)$ ,  $\lambda$  and  $\nu$  are KKT multipliers for the equations and bounds, respectively, and  $e$  is a vector of ones. To solve this nonlinear KKT system, IPOPT uses an exact Newton method with a novel filter line search method and efficient sparse linear solvers.

#### Optimization problem for Natural Gas Plant

To demonstrate the above optimization for switching between steady states, we minimize the offset between ethane recovery and a set point value. Here, the optimization variables are demethanizer top pressure ( $P_{top}$ ) and flowrate fraction derived through the bypass valve in cryogenic heat exchangers (XG). The dynamic optimization problem has been formulated in AMPL within a simultaneous approach (Waechter and Biegler, 2006). For accurate approximations with guaranteed convergence properties, even for DAE high index problems, Radau collocation was implemented (Biegler 2010) to discretize the DAE model. We apply this approach to the following dynamic optimization problem:

$$\min \int_0^{t_f} (\eta_{ethane} - \eta_{SP})^2 dt$$

st.

$$\{DAE Model\}$$

$$15 \leq P_{TOP} \leq 22 \text{ (bar)}$$

$$99 \leq Q_{REB} \leq 200 \text{ (kJ/min)}$$

$$0 \leq x_G \leq 1.$$

$$0 \leq x_{B,CH4} \leq 0.008$$

$$\overline{f_{i,CO2}^V} \leq 0.80 f_{i,CO2}^S; i = 1, \dots, 4$$

$$Ts_k - Tt_{k+1} \geq \Delta T_{min}; k = 1, \dots, N_{cells1} - 1$$

$$Ts_k - Tt_{IN1} \geq \Delta T_{min}; k = N_{cells1}$$

$$Ts_j - Tt_{j+1} \geq \Delta T_{min}; j = 1, \dots, N_{cells2} - 1$$

$$Ts_j - Tt_{IN} \geq \Delta T_{min}; j = N_{cells2}$$

$$Ts_{m,IN} \geq Ts_{m,1}; m = 1, 2$$

$$Ts_{m,i} \geq Ts_{m,i+1}; i = 1, \dots, N_{cellsm} - 1; m = 1, 2$$

$$Tt_{m,i} \geq Tt_{m,i+1}; i = 1, \dots, N_{cellsm} - 1; m = 1, 2$$

$$Tt_{m,N_{cellsm}} \geq Tt_{m,IN}; m = 1, 2$$

$$z(t=0) = z_0; y_L \leq y \leq y_U; z_L \leq z \leq z_U$$

## Numerical results

The dynamic optimization of the entire plant is performed to switch to a steady state with higher ethane recovery. Control variables, corresponding to top pressure in the demethanizer column and the bypass fraction to the first cryogenic heat exchanger, were computed along a time horizon of 100 minutes. A full discretization has been carried out with 15 finite elements with two collocation points, rendering an NLP with 82320 variables and 81720 equality constraints. This led to a reasonably accurate solution. Further extensions that deal with error bounding strategies (see Biegler, 2010) are also planned for future work.

To improve computational performance, we provided exact first and second derivatives along with initializations of the primal variables and bound multipliers through the AMPL environment. In addition, we used the MA57 solver with Metis. Among the IPOPT options, better results have been obtained with the adaptive barrier update and warm starts. The entire plant optimization has been performed in 51 CPUs on an Intel DuoCore 2.2 GHz personal computer.

For this case, ethane recovery is increased from 67% for an initial pressure of the demethanizer of 18 bar, to 75.20% at 15.80 bar, and to an increase in the residual gas flow rate bypassed in the first heat exchanger from 26% to 30%. Figure 3 shows optimal profiles for the control

variables: the top demethanizer pressure and bypass fraction. Figure 4 shows the turboexpander outlet temperature profile, which is decreased by an increase of the expansion ratio (TEinlet pressure/Demethanizer top pressure). This leads to the increase in ethane recovery, which is also shown in this figure. Figures 5 and 6 show spatial and temporal profiles for shell side temperature and pressure in the cryogenic heat exchanger where partial condensation takes place. A spatial discretization of six cells has been considered. It can be seen that the increase in the bypassed residual gas flow rate renders a slight increase in the new steady state feed gas outlet temperature (from 213.6 to 214.5 K). Figure 7 shows a decrease in inlet residue gas temperature (from 193 to 191K), associated to the demethanizer column temperature decrease; it also shows an increase in its outlet value in the new steady state due to the warmer feed gas conditions associated to the increase in bypassed residue gas in the second cryogenic heat exchanger. Figure 8 shows the warmer final conditions in the feed gas associated to the increase in bypassed residue gas flow rate.

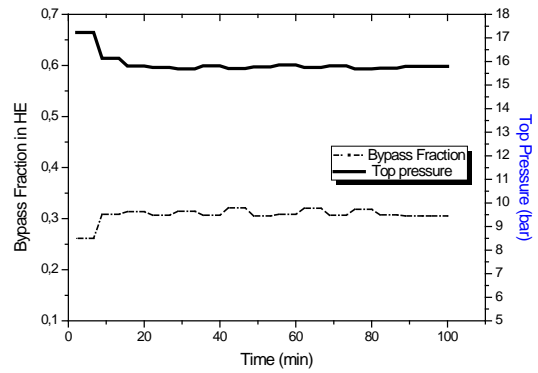


Figure 3. Bypass fraction in cryogenic heat exchangers and demethanizer top pressure (control variables)

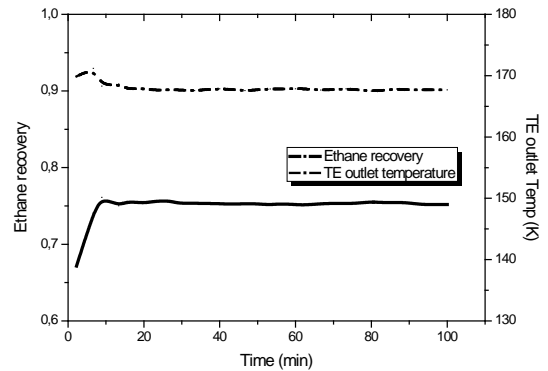


Figure 4. Optimal turboexpander outlet temperature (K) and ethane recovery

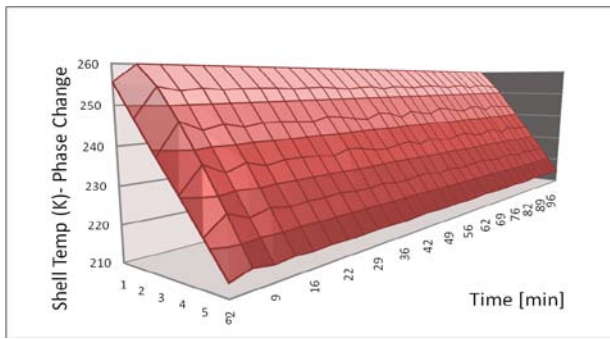


Figure 5. Heat exchanger with phase change: Shell-side spatial (6 cells) & temporal temperature profile (feed gas)

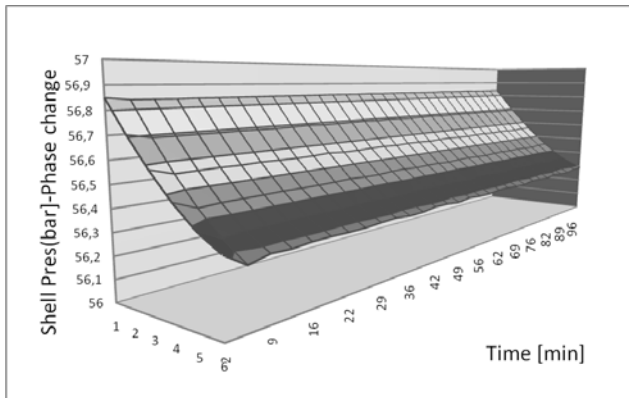


Figure 6. Heat exchanger with phase change: Spatial (6 cells) and temporal pressure profile on shell side (feed gas)

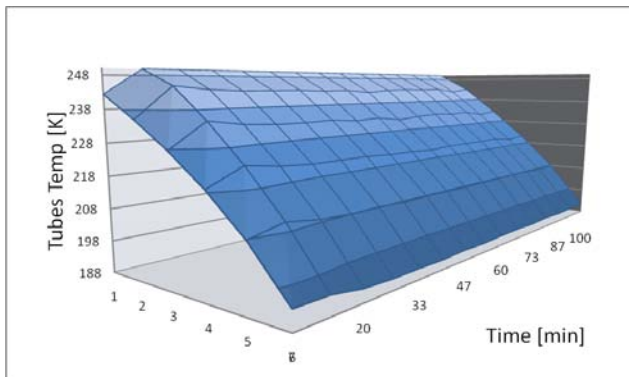


Figure 7. Heat exchanger with phase change: Tube-side spatial (6 cells) & temporal pressure profile (residue gas)

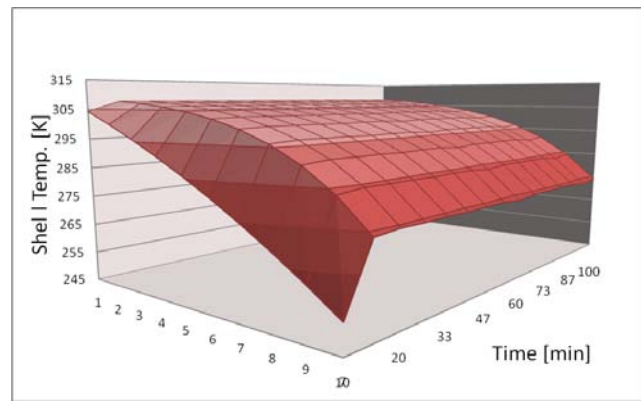


Figure 8. Cryogenic heat exchanger with no phase change: Shell-side spatial (10 cells) & temporal temperature profile

## Conclusions

This study develops a dynamic optimization formulation to determine transition profiles for changes in steady state conditions for a natural gas processing plant, a highly energy integrated process. Here we consider the formulation of first principles models for process units within a simultaneous dynamic optimization approach. The resulting NLP problem has a large number of variables and equations, but the application of Newton-based Interior Point methods, as well as appropriate handling of the Jacobian and Hessian structure within IPOPT (Wächter and Biegler, 2006) allows for efficient and accurate solution with a considerable reduction of CPU time. This study paves the way for the use of rigorous models for energy minimization, maximization of product recovery and extension within a nonlinear model predictive control environment, which will be investigated in future studies.

## Acknowledgements

The authors gratefully acknowledge financial support from the National Research Council (CONICET), Universidad Nacional del Sur and ANPCYT, Argentina.

## References

- Biegler, L.T., V.M. Zavala (2008), Large-scale nonlinear programming using IPOPT: An integrating framework for enterprise-wide dynamic optimization. *Computers and Chemical Engineering* 33 (2009) 575–582
- Biegler, L. T. (2010), *Nonlinear Programming: Concepts, Algorithms and Applications to Chemical Processes*, SIAM, Philadelphia, PA
- Cervantes A. M., L. T. Biegler (1998). Large-scale DAE optimization using a simultaneous NLP formulation. *AICHE Journal*, 44, 1038-1050.
- Diaz, S., S. Tonelli, A. Bandoni, L.T. Biegler (2003), “Dynamic optimization for switching between steady states in cryogenic plants”, *Found Comp Aided Process Oper* 4, 601-604.

- Mandler J.A. (2000). "Modelling for control analysis and design in complex industrial separation and liquefaction processes", *J. Process Control*, 10, 2, 167-175.
- Raghunathan, A., M.S. Diaz, L.T. Biegler (2004). "An MPEC Formulation for Dynamic Optimization of Distillation Operations", *Computers & Chemical Engineering*, 28, 2037-2052.
- Rodriguez, M., (2009) "Dynamic Modeling And Optimization of Cryogenic Separation Processes", PhD Dissertation, Universidad Nacional del Sur, Bahia Blanca, Argentina.
- Rodríguez, M., M. S. Diaz, (2007), "Dynamic Modelling And Optimisation of Cryogenic Systems", *Applied Thermal Engineering* (ISSN 1359-4311), 27, 1182-1190.
- Rodriguez, J. I. Laiglecia, P. M. Hoch, M. S. Diaz (2010) "Dynamic optimization of an Intensive Energetically Integrated Large-Scale Process," *Computer Aided Chemical Engineering*, Volume 28, Pages 469-474
- Schiesser, W.E., (1991), *The Numerical Method of Lines*, San Diego, CA: Academic Press
- Soave G. Equilibrium Constants for a Modified Redlich-Kwong Equation of State. *Chem. Eng. Sci.* 1972; 27: 1197-1203.
- Vinson, D.R., (2006), Air separation control technology, *Computers & Chemical Engineering*, 30, 10-12, 1436-1446.
- Waechter, A., Biegler, L.T. (2006), "On the Implementation of an Interior Point Filter Line Search Algorithm for Large-Scale Nonlinear Programming," *Mathematical Programming*, 106, 1, pp. 25-57